The latest version is at http://www.jbc.org/cgi/doi/10.1074/jbc.M116.719039

Formation of Functional Heterodimers by TREK-1 and TREK-2 Two-pore Domain Potassium Channel Subunits

Miklós Lengyel, Gábor Czirják and Péter Enyedi

From the Department of Physiology, Semmelweis University, Budapest, Hungary

Running title: Heterodimerization of TREK-1 and TREK-2 Subunits

To whom correspondence should be addressed: Péter Enyedi, Department of Physiology, Semmelweis University, P.O. Box 2, H-1428 Budapest, Hungary; E-mail: enyedi.peter @med.semmelweis-univ.hu; Tel.: +36 1 459 1500/60431; fax: +36 1 266 7480.

Keywords: Potassium channel, Electrophysiology, Patch clamp, Plasma membrane, Pharmacology, Ion channel heteromerization, Spadin, Ruthenium red, KCNK2, KCNK10

Abstract

Two-pore domain (K_{2P}) potassium channels are the major molecular correlates of the background (leak) K^+ current in a wide variety of cell types. They generally play a key role in setting the resting membrane potential and regulate the response of excitable cells to various stimuli. K_{2P} channels usually function as homodimers and only a few examples of heteromerization have been previously reported. Expression of the TREK (TWIK-related K^+ channel) subfamily members of K_{2P} channels often overlaps in neurons and in other excitable cells. Here we demonstrate that heterologous coexpression of TREK-1 and TREK-2 subunits results in the formation of functional heterodimers. Taking advantage of a tandem construct (in which the two different subunits were linked together to enforce heterodimerization) we characterized the biophysical and pharmacological properties of the TREK-1/TREK-2 current. The heteromer was inhibited by extracellular acidification and by spadin similarly to TREK-1, while its ruthenium red sensitivity was intermediate between TREK-1 and TREK-2 homodimers. The heterodimer has also been distinguished from the homodimers by its unique single channel conductance. Assembly of the two different subunits was confirmed by coimmunoprecipitation of epitope tagged TREK-1 and TREK-2 subunits, coexpressed in *Xenopus* oocytes. Formation of TREK-1/TREK-2 channels was also demonstrated in native dorsal root ganglion neurons indicating that heterodimerization may provide greater diversity of leak K^+ conductances also in native tissues.

Introduction

Heteromerization of subunits is a widespread mechanism for increasing diversity in voltage-gated (K_v) and inwardly-rectifying (K_{ir}) K^+ channel subfamilies. The resulting heteromers are typically characterized by different biophysical and regulatory properties from the homomers of the parent subunits. Certain K_v or K_{ir} (e.g. K_v8.1 or K_{ir}5.1) subunits cannot form functional homomers on their own, however, via heteromerization they can also gain important physiological function (for review see (1)); deletion or mutations of their genes has been associated with genetic diseases and pathophysiological conditions (for example (2-4)).

Two-pore domain (K_{2P}) K^+ channels are the molecular correlates of background (leak) K^+ currents. The mammalian K_{2P} family consists of 15 different members, which are grouped into 6 subfamilies: TWIK (Tandem of pore domains in a Weak Inward rectifying K^+ channel), TREK (TWIK-Related K^+ channel), TASK (TWIK-related Acid-Sensitive K^+ channel), TALK (TWIK-Related Alkaline pH-activated K^+ channel), THIK (Tandem pore domain Halothane-Inhibited K^+ channel) and TRESK (TWIK-Related Spinal cord K^+ channel) (for review see (5)). In contrast to K_v and K_{ir} tetramers containing one pore domain per subunit,

K_{2P} subunits possess two pore domains and accordingly dimerize to form functional channels. Only a few examples of heterodimerization have been described in the K_{2P} channel family so far. The first example, heteromerization of TASK-1 with TASK-3 was characterized in our laboratory (6). The preferentially formed TASK-1/TASK-3 heterodimer has since been detected in several native cells (7-12). The heterodimer plays a role in fine tuning the resting membrane potential and the sensitivity of the cells to physiological stimuli (extracellular pH changes, agonists of G_q-protein coupled receptors) in glomus cells, cerebellar granule neurons and motoneurons. Subsequently, further heterodimers of K_{2P} channel subunits have been recognized. The heterodimerization of THIK-1 and THIK-2 has been reported, apparently THIK-1 was able to counteract the endoplasmic retention of THIK-2 (13). Another K_{2p} channel interaction (in which the partner subunits belong to different subfamilies), the heteromerization of the silent TWIK-1 subunit with TASK-1 (or TASK-3) has recently been revealed. Properties of the heteromer were analyzed in detail in cerebellar granule cells and also in a heterologous expression system; TWIK-1 was found to confer SUMOylation sensitivity to the heteromer (14). While in this study TWIK-1 and TREK-1 coexpression served as a negative control, as no sign of interaction was found between these two subunits, TWIK-1/TREK-1 heteromerization was reported by another group in hippocampal astrocytes (15). Quite unexpectedly, activation of a G_i-protein coupled receptor was claimed to convert the heterodimer into an anion conductive channel (15); the authors have suggested that the binding of the βγ subunits to the heterodimer induces channel pore dilation resulting in glutamate permeability. This intriguing hypothesis, however, remains controversial and has yet to be proven experimentally.

The closely related TREK-1 and TREK-2 channels (encoded by the KCNK2 and KCNK10 (Potassium channel subfamily K member 2 and 10) genes) are thermo- and mechanosensitive, they are activated by volatile anesthetics, intracellular acidosis, arachidonic acid and also similarly modulated by a wide variety of signaling cascades initiated by activation of G-protein coupled receptors. On the other hand, TREK-1 and TREK-2 channels are regulated differently by extracellular (EC) acidification: TREK-1 is inhibited, while TREK-2 is activated (16,17). TREK-1 is inhibited by the sortilin-derived neuropeptide spadin, while TREK-2 is insensitive to spadin (18,19). Recently we have described the differential pharmacological effect of the polycationic dye ruthenium red (RR) on TREK channels: TREK-2 is potently inhibited by the dye, while TREK-1 is insensitive to RR (20). The overlapping expression of the two TREK subunits raises the possibility of heteromerization in native tissues, which may result in a channel with new attributes (e.g. different single channel conductance, pH sensitivity and distinct regulatory profile). In this paper, by applying pharmacological tools combined with single channel measurements, we demonstrate that TREK-1 and TREK-2 subunits form functional heterodimers when coexpressed in *Xenopus laevis* oocytes, HEK293T cells and isolated dorsal root ganglion neurons. The properties of the heterodimer proved to be different from those of the homodimers, thus further expanding the diversity of leak K^+ currents.

Experimental procedures

Materials:

Chemicals of analytical grade were purchased from Sigma (St. Louis, MO, USA), Fluka (Milwaukee, WI, USA) or Merck (Whitehouse Station, NJ, USA). Enzymes and kits for molecular biology applications were purchased from Ambion (Austin, TX, USA), Thermo Scientific (Waltham, MA, USA), New England Biolabs (Beverly, MA, USA) and Stratagene (La Jolla, CA, USA). The sortilin-derived peptide spadin was synthesized by the MTA-ELTE Research Group of Peptide Chemistry (Budapest, Hungary), dissolved in distilled water and stored as 1 mM stock solution at -20 ^{o}C.

Molecular biology:

Channel constructs: The plasmid coding mouse TREK-1 (mTREK-1) channel was kindly provided by Professor M. Lazdunski and Dr. F. Lesage. The cloning of mouse TREK-2 channel from mouse brain has been described previously (21). For expression in mammalian cell lines, the coding sequences of TREK-1 and TREK-2 were subcloned into the pcDNA3.1 expression vector. For coexpression of TREK-1 and TREK-2 channel

subunits in the same cell the two channel subunits were linked by a viral peptide, T2A, which displays a self-cleaving property during translation (22) and was shown to ensure equimolar separate expression of the two proteins (23).

Assembly of the TREK-2/TREK-1 concatenated (tandem) construct: the coding sequence of TREK-2 (without the stop codon) and that of TREK-1 (without the start codon) were amplified from mTREK-2-pEXO and mTREK-1-pEXO plasmids by PCR, respectively. The TAA stop codon of the TREK-2 subunit and the ATG start codon of the TREK-1 subunit were replaced with a unique MunI restriction enzyme sites. This introduced a two-amino acid (glutamate and leucine) linker between the two concatenated subunits after final ligation into a pXEN vector between Eco81I and XbaI restriction sites.

Cloning of TREK mutants: The 'long' version of mTREK-1 (mTREK-1-L), from which translation can only initiate from the first ATG codon of the mTREK-1 coding sequence was created by mutating the alternative translation initation site (M58) of mTREK-1 to isoleucine (24) with QuikChange site-directed mutagenesis kit (Stratagene, La Jolla, CA, USA) according to the manufacturer's instructions. The 'long' version of TREK-2 (M55L and M67L), used in coimmunoprecipitation experiments was constructed with a similar approach. The 'short' version of mTREK-2 (mTREK-2-S), where translation can only initiate from the last downstream start codon of the wild type TREK-2 sequence, was created by amplifying the coding sequence of mTREK-2-pEXO plasmid without the first 66 amino acids of the N-terminus. The PCR product was inserted into pXEN vector between Eco81I and XbaI restriction sites.

During the assembly of TREK-2-S/TREK-1-L tandem construct the same strategy was followed as detailed above at the TREK-2/TREK-1 construct, however, the templates of the PCR reactions were replaced by the mutant subunits.

TREK-1-L and TREK-2-L subunits were labelled with epitope tags (V5 and FLAG respectively) using PCR. The fidelity of all the constructs generated by PCR was verified by automated sequencing.

cRNA synthesis:

The plasmids coding wild type, tagged or mutant channel constructs were linearized with NotI, XhoI or XbaI restriction enzymes. These templates were used for *in vitro* RNA synthesis. RNA was synthesized using the Ambion mMESSAGE mMACHINE™ T7 *in vitro* transcription kit (Ambion, Austin, TX). The structural integrity of the RNA was checked on denaturing agarose gels and RNA was quantified spectrophotometrically.

Animals, tissue preparation, Xenopus oocyte microinjection and isolation of dorsal root ganglion neurons:

Xenopus laevis oocytes were prepared as previously described (6). Oocytes were injected 1 day after defolliculation with 2-6 ng RNA per oocyte for two electrode voltage clamp and membrane preparation experiments while 0.025-0.5 ng RNA per oocyte was used for single channel recordings. Fifty nanoliters of the appropriate RNA solution was delivered with Nanoliter Injector (World Precision Instruments, Saratosa, FL). Dorsal root ganglion (DRG) neurons were isolated from 3 months old FVB/Ant mice obtained from the Institute of Experimental Medicine of the Hungarian Academy of Sciences (Budapest, Hungary). Their preparation and culturing was previously described (20). All the animal experiments were approved by the Animal Care and Ethics Committee of Semmelweis University (approval ID: XIV-I-001/2154-4/ 2012).

Electrophysiology:

Two-electrode voltage clamp experiments were performed 2-3 days after the microinjection of cRNA into *Xenopus* oocytes, as previously described (25). The holding potential was -75 mV. Background K^+ currents were measured at the end of 300 ms long voltage steps to −100 mV applied every 4 s. Low [K^+] solution contained (in mM): NaCl 95.4, KCl 2, $CaCl_2$ 1.8, HEPES 5. High [K^+] solution contained 40 mM K^+ (38 mM Na^+ of the low [K^+] solution was replaced with K^+). The pH of the solutions was adjusted to 8.5 or 6.5 with NaOH on the day of the experiment. RR was diluted in high [K^+] solution before the experiment from a 10 mM stock solution in 0.1 M ammonium acetate. Experiments were carried out at room temperature (21°C). Solutions were applied using a gravity-driven perfusion system. Data were analyzed by

pCLAMP 10 software (Molecular Devices, Sunnyvale, CA, USA).

For patch clamp experiments pipettes were pulled from thick-walled borosilicate glass (Standard Glass Capillaries, 4 in., 1.2 / 0.68 OD/ID, Filament/Fire Polished (Item number: 1B120F-4) from World Precision Instruments, Sarasota, Florida) by a P-87 puller (Sutter Instrument Co., Novato, CA, USA) and fire polished. Pipettes were filled with pipette solution and connected to the headstage of an Axopatch-1D patch clamp amplifier (Axon Instruments, Inc., Foster City, CA, USA). Experiments were carried out at room temperature (21°C). Solutions were applied using a gravity-driven perfusion system. Data were digitally sampled by Digidata 1200 (Axon Instruments, Inc.). Data were analyzed by pCLAMP 10 software.

Whole-cell patch clamp experiments were performed on HEK293T cells (ATCC, Manassas, VA) 1-2 days after transfection. Cells were seeded at a density of 20.000-50.000 cells per 35 mm dish 48h prior to transfection in 10% bovine serum in Dulbecco's modified Eagle's medium (DMEM). HEK293T cells were co-transfected with plasmids encoding TREK-1, TREK-2 or TREK-1-T2A-TREK-2 and a plasmid coding CD8 using LipofectAMINE2000 transfection reagent (Invitrogen) and UltraMEM Reduced Serum Medium (Lonza). Transfected cells were identified using anti-CD8 Dynabeads (Thermo Fisher Scientific). Cut-off frequency of the eight-pole Bessel filter was adjusted to 200 Hz, data were acquired at 1 kHz. Pipette solution contained (in mM): 140 KCl, 3 $MgCl_2$, 0.05 EGTA, 1 Na_2-ATP, 0.1 Na_2-GTP and 10 HEPES. Low $[K^+]$ solution contained (in mM): 140 NaCl, 3.6 KCl, 0.5 $MgCl_2$, 2 $CaCl_2$, 11 glucose and 10 HEPES (pH adjusted to 7.4 with NaOH). High $[K^+]$ contained 30 mM KCl (26.4 mM Na^+ of the low $[K^+]$ solution was replaced with K^+). The pH of the high $[K^+]$ solution was adjusted to 7.4 or 6.4 with NaOH.

Single channel currents were recorded from *Xenopus laevis* oocyte membrane patches 2 days after injection or from DRG neurons 1-2 days after isolation. Oocytes were devitellinized manually in modified Barth's saline after a brief exposure to hyperosmotic conditions (500 mOsm). Cut-off frequency of the eight-pole Bessel filter was adjusted to 2 kHz, data were acquired at 20 kHz. Data were analyzed by pCLAMP 10 software. Recordings were low-pass filtered at 200 Hz with pCLAMP10 software before analysis.

On inside-out membrane patches single channel currents were recorded at a membrane potential of +60 mV. The pipette solution contained (in mM): 136 NaCl, 4 KCl, 5 EGTA, 1 $MgCl_2$ and 10 HEPES (pH 7.4 adjusted with NaOH). Pipette resistances were 3-7 MΩ when filled with pipette solution. Bath solution contained (in mM): 140 KCl, 5 EGTA, 1 $MgCl_2$ and 10 HEPES (pH 7.1 adjusted with KOH). The charge carrier of the currents recorded was verified as K^+ in all patches by transiently substituting the bath solution with a K^+-free bath solution (140 NaCl, 5 EGTA, 1 $MgCl_2$ and 10 HEPES, pH 7.1 adjusted with NaOH).

During the measurements on outside-out membrane patches single channel currents were measured at a membrane potential of -60 mV. The pipette solution contained (in mM): 140 KCl, 5 EGTA, 1 $MgCl_2$ and 10 HEPES (pH 7.1 adjusted with KOH). Pipette resistances were 3-6 MΩ when filled with pipette solution. Bath solution contained (in mM): 140 KCl, 5 EGTA, 1 $MgCl_2$ and 10 HEPES (pH adjusted to 7.4 or 6.4 with KOH). RR or spadin were dissolved in the bath solution on the day of the measurement. Verification of the charge carrier as K^+ was done by determining the reversal potential of the current.

Data were analyzed to obtain amplitude histograms and channel activity (NP_o, where N is the number of channels in the patch, and P_o is the probability of a channel being open). Single channel current amplitudes were determined from the amplitude histograms. NP_o was determined from 30-60 seconds of current recording.

Statistics:

Results are expressed as means±S.E.M. Statistical significance was determined using Student's t test for independent samples or ANOVA followed by Tukey's post hoc test. The difference was considered to be significant at $p<0.05$. All statistical calculations were done using Origin8 (OriginLab Corporation, Northampton, MA).

Pull-down experiments:

Membrane fraction was prepared from *Xenopus laevis* oocytes coinjected with wild type or tagged TREK-1 and TREK-2 cRNA after two days of expression. All preparation steps were performed

at 4ºC. Thirty oocytes in each group were homogenized in a Potter homogenizer in buffer H containing (in mM) 90 NaCl, 1 $MgCl_2$, 10 HEPES (pH. 7.9), and a protease inhibitor cocktail. The lysate was centrifuged at 1.000 g for 10 min. The supernatant was saved and the centrifugation step repeated. The 'low speed' supernatant was centrifuged at 16.000 g for 20 min, the pellet (containing the membrane fraction) was washed with buffer H and resuspended in solubilizing (S) solution containing (in mM) NaCl 250, EDTA 2, HEPES 50 (pH 7.4), glycerol (10%), Triton-X 100 1% and a protease inhibitor cocktail.

Solubilization for 3 hours was followed by centrifugation (16.000 g, 20 min) and the supernatant (solubilized membrane fraction) was added to equilibrated 30 µl immunaffinity agarose gel containing goat polyclonal Ab to V5 tag (1229, Abcam, Cambridge, UK). Reactions were incubated overnight by rotating the slurry. The resin was pelleted at 5.000 g for 1 min. and washed three times with solution S. Proteins were eluted with SDS sample buffer, aliquots (equivalent with the membrane fraction of 1 oocyte) were heated to 90ºC for 15 min and were subjected to SDS-polyacrylamide gel electrophoresis and Western blot. Interaction between TREK-1-V5 and TREK-2-FLAG subunits was detected using an anti-FLAG M2 mouse monoclonal antibody (F3165, Sigma-Aldrich, St. Louis, MO) 1:10.000 and a horseradish peroxidase-conjugated anti-mouse IgG from goat 1:10.000 (R05071), Advansta, Menlo Park, CA).

Results

Construction of a functional TREK-2/TREK-1 tandem channel

We have previously shown that functional TREK-2/TREK-2 tandem channels can be engineered by concatenating two identical coding regions (20). Electrophysiological and pharmacological properties of these tandem constructs were indistinguishable from the native, posttranslationally dimerized TREK-2 channels. In the present experiments, the C-terminus of TREK-2 was joined to the N-terminus of TREK-1 via a two amino acid linker. Expression of this construct in *Xenopus laevis* oocytes resulted in a potassium conductance as measured by the two-electrode voltage clamp technique. Assembly of the covalently linked subunits into a heterodimer was indicated by the absence of leak K^+ current expression by a mutant tandem TREK-2/TREK-1-mut construct in which the signature sequence in the first pore domain of the TREK-1 subunit was changed from GFG to GFE (the K^+ current of the oocytes expressing the mutant tandem was 6% compared to those expressing the wild type TREK-2/TREK-1 tandem (n=5); this current was in the range of non-injected oocytes). Accordingly the tandem channel was considered as a plausible model for heteromerization, and it has been used to predict the pharmacological properties of the heterodimer composed of native TREK-1 and TREK-2 subunits.

The TREK-2/TREK-1 tandem channel has intermediate RR sensitivity and is inhibited by extracellular acidification

Pharmacological effects of extracellular acidification and RR on different TREK currents were determined in *Xenopus* oocytes at -100 mV in high (40 mM) [K^+] solution. In good accordance with the previous results (16,17), TREK-1 was inhibited by changing the pH from 8.5 to 6.5 (49.7±4.3% inhibition, n=10, Fig. 1.A and D), whereas TREK-2 was substantially activated by the same treatment (the current increased to 243.3±17.5% of the value measured at pH 8.5, n=6, Fig. 1.B and D). The TREK-2/TREK-1 tandem construct was inhibited by EC acidification (by 32.7±1.4%, n=8, Fig. 1.C and D). This degree of inhibition of the tandem channel is not significantly different from that of TREK-1 homodimer (p=0.34), suggesting that the inhibitory mechanism responsible for the pH sensitivity of TREK-1 is dominant over the activating effect on TREK-2 subunit.

As we have recently reported (20), RR polycation unambiguously differentiates between the K^+ currents of TREK-1 and TREK-2 homodimeric channels on the basis of a single amino acid residue difference in the closely related subunits (negatively charged aspartate in TREK-2, neutral isoleucine in TREK-1). In order to test whether EC pH influences the inhibition elicited by RR, the oocytes expressing TREK-2 were

challenged with the polycationic dye (3 μM) in two different solutions adjusted to pH 6.5 or 8.5. TREK-2 current was reduced by 76±5% at pH 6.5 and 81±3% at pH 8.5, respectively (p=0.39), indicating that EC pH does not affect the inhibition evoked by RR (data not shown). Therefore, in further experiments, the effects of acidification and RR were measured in the same oocyte by reducing pH (from 8.5 to 6.5), and subsequently applying RR (30 μM) in the acidified solution. TREK-2 current was potently inhibited by RR (85.9±2.3% inhibition, n=6, Fig. 1.B and E), while the RR sensitivity of TREK-1 was marginal (9.6±2.3%, n=10, Fig. 1.A and E). The tandem channel was characterized by intermediate RR sensitivity (49.4±4.3% inhibition, n=8, Fig. 1.C and E). This intermediate inhibition of the tandem channel by high (30 μM) concentration of RR was significantly different from both of the homodimeric channels ($p<10^{-6}$).

Thus we have identified two pharmacological properties of TREK-2/TREK-1 tandem channel, which were inherited in different manners from the parent subunits. TREK-2/TREK-1 tandem was nearly identical to TREK-1 with respect to acidification but the response of the tandem channel to RR was intermediate between TREK-1 and TREK-2 homodimers. In order to present this graphically, the effects of decreased EC pH and RR application on TREK currents were plotted against each other (one point corresponds to one oocyte, Fig. 2.A). The data point averages of TREK-1 and TREK-2 homodimers were connected with a straight line. The data points of oocytes expressing TREK-2/TREK-1 tandem channel clearly deviated from the connecting line (Fig. 2.A). This illustrates that the covalent linkage of the different subunits resulted in an offspring which inherited the pharmacological properties of the parent channels asymmetrically. This asymmetrical inhibitory profile was exploited in the further experiments to investigate the heterodimers formed by separate TREK-1 and TREK-2 subunits.

Coexpression of TREK-1 and TREK-2 subunits results in TREK-1/TREK-2 heterodimer formation

Covalent linkage of TREK-1 and TREK-2 subunits forces the formation of functional „heterodimeric" channels, which are characterized by pharmacological properties different from the homodimers. In order to test whether separate TREK-1 and TREK-2 subunits can also coassemble spontaneously, oocytes were injected with different ratios of TREK-1 and TREK-2 cRNA. The pH and RR sensitivities of the resulting TREK currents were determined and plotted in the way established above (Fig. 2.B). Theoretically, if the two coexpressed subunits did not form heterodimers then two independent populations of homodimers would be produced in each cell. In this case, the data points corresponding to the oocytes would fall on the line connecting the averages of TREK-1 and TREK-2 homodimers, and the exact position of the data point on the line would reflect the ratio of the two coexpressed homodimeric channel types. However, data points from the coexpression experiment clearly deviated from the connecting line, and approximated the position of tandem channel data points, depending on the ratio of TREK-1 to TREK-2 expression. This suggests that functional heterodimers were spontaneously constituted by individual TREK-1 and TREK-2 subunits.

Verification of heterodimer formation by measuring single channel conductance

Another approach to distinguish TREK-1, TREK-2 and the heteromeric channel is to measure their characteristic single channel conductance. However, this approach is complicated by the fact that multiple conductance levels arise for both TREK-1 and TREK-2 channels due to alternative translation initiation (24,26). In order to overcome this heterogeneity, mutant channels were constructed. On the basis of literature data, the isoforms of native TREK-1 and TREK-2 with maximum difference between their single channel conductance were produced. N-terminal deleted 'short' TREK-2 (TREK-2-S) was translated only from the downstream native initiation site, whereas in 'long' M58I mutant TREK-1 (TREK-1-L) the additional site of translation initiation was disabled by mutation. In this way, each channel was translated starting only from one initiation site and multiple conductance levels have been eliminated. A version of the tandem channel (TREK-2-S/TREK-1-L) was also constructed from the modified subunits. The pH and RR sensitivities of the mutants were checked and found to be similar to

those of the wild type channels. When TREK-1-L and TREK-2-S were coexpressed, the sensitivity of the macroscopic current to acidification and RR showed a similar pattern as that obtained with wild type TREK-1 and TREK-2 (data not shown).

Single channel currents were recorded from inside-out membrane patches of oocytes expressing TREK-1-L, TREK-2-S or TREK-2-S/TREK-1-L tandem constructs. Unitary currents and single channel conductances were calculated from 30-60 second periods of the recordings. Under our experimental conditions, the single channel conductance of TREK-1-L was 39.2±2.7 pS (n=6 patches, Fig. 3.A). TREK-2-S had a large conductance of 148.8±4.2 pS (n=7 patches, Fig. 3.B). The conductance of TREK-2-S/TREK-1 tandem channel was 83.5±5.0 pS, an intermediate value (n=8 patches, Fig. 3.C). The difference between the conductance of the homodimers and the tandem channel was statistically significant ($p<0.01$). Thus the TREK-1-L/TREK-2-S heterodimer can be distinguished from both TREK-1-L and TREK-2-S based on its single channel conductance (Fig. 3.D).

Patches from oocytes coexpressing TREK-1-L and TREK-2-S contain heterodimeric channels

Xenopus oocytes were injected with different ratios of TREK-1-L and TREK-2-S cRNA. Unitary currents and single channel conductances were calculated from patches containing one or two channels and plotted against the different RNA ratios (Fig. 4.). The recorded channels clearly formed three distinct groups. Based on the single channel conductances in Fig. 3., the three groups correspond to TREK-1-L homodimers (circles), TREK-2-S homodimers (triangles) and TREK-1-L/TREK-2-S heterodimers (diamonds). Increasing the amount of TREK-2-S cRNA, while keeping the amount of total cRNA constant (0.025 ng cRNA/oocyte) lead to an increased amount of heterodimer and TREK-2-S homodimer formation (see Fig. 4., compare the column marked 1:1 to the columns marked 1:4 and 1:12). Thus the formation of TREK-1/TREK-2 heterodimers was confirmed at the single channel level.

RR inhibits single TREK-2-S and TREK-2-S/TREK-1-L channels

In order to relate characteristic channel conductances to the specific pharmacological profiles, TREK-1-L, TREK-2-S and TREK-2-S/TREK-1-L tandem single channel currents were measured in the outside-out configuration. Channel activity (NP_o) was determined before, during and after application of 30 μM RR to the bath solution. The dye had a small inhibitory effect on TREK-1-L channel activity (-19±3 %, n=4 patches) but efficiently inhibited TREK-2-S (-90±6%, n=7 patches, Fig. 5.A and B). In the case of TREK-2-S, a decrease was also observed in the single channel unitary current, but it was not statistically significant ($p=0.066$). The inhibition of the TREK-2-S/TREK-1-L tandem channel activity by RR (-55±11%, n=4 patches) was greater than the inhibition of TREK-1-L, but less than the effect of the dye on TREK-2-S (Fig. 5.C). The effect of RR was reversible. The different degree of inhibition between the homodimers and the tandem channel was statistically significant ($p<0.025$). Thus the effect of RR on TREK single channel currents proved to be consistent with that observed at the whole cell level.

Extracellular acidification inhibits single TREK-1-L and TREK-2-S/TREK-1-L channels and activates TREK-2-S

TREK-1-L, TREK-2-S and TREK-2-S/TREK-1-L tandem channels were expressed in *Xenopus* oocytes. Single channel currents were then recorded from outside-out membrane patches. Channel activity was determined before, during and after acidification (from pH 7.4 to 6.4) of the bath solution. The effect of the acidic extracellular pH on single TREK channels was similar to its effect on TREK channels observed at the whole cell level as seen on Fig. 1. Extracellular acidification had a quantitatively similar inhibitory effect on TREK-1-L (-50±8%, n=5 patches) and TREK-2-S/TREK-1-L tandem activity (-42±20%, n=4 patches, Fig. 6.A and C). TREK-2-S channel activity (Figure 6.B) was augmented by acidification (192±19%, n=5 patches). The effect of the pH change was reversible. Modification of the extracellular pH is a potential tool to separate homodimeric TREK-2

channels, where NP_o is increased by EC acidification, from TREK-1 homodimers and heterodimers (where NP_o is decreased by low pH).

Spadin inhibits single TREK-1 and TREK-2-S/TREK-1-L channels

The effect of spadin on TREK channels was measured on membrane patches expressing TREK-1-L, TREK-2-S and TREK-2-S/TREK-1-L tandem channels in the outside-out configuration. Channel activity was determined before, during and after the addition of spadin (1 μM) to the EC solution. Spadin is a potent inhibitor of TREK-1 channel activity (NP_o was inhibited by 60±11.2%, n=4 patches, Fig. 7.A), while TREK-2 activity was not influenced by the application of the peptide (101±14.4% remaining current, n=4 patches, Fig. 7.B). Interestingly, TREK-2-S/TREK-1-L tandem channel was also inhibited by the peptide (Fig. 7.C, 85±12%, n=5 patches). The difference in the degree of inhibition between TREK-2-S homodimer and TREK-2-S/TREK-1-L was statistically significant ($p<0.005$), while the inhibition of TREK-1-L and the tandem channel by spadin were not different ($p=0.38$, Fig. 7.D). The inhibitory effect of the peptide was reversible on both TREK-1-L and TREK-2-S/TREK-1-L. These data indicate that the association of TREK-1 subunit to the otherwise spadin-resistant TREK-2 confers susceptibility to the peptide, and the process of heteromerization may increase the sensitivity of the background K^+ current to spadin in the cells which coexpress TREK-1 and TREK-2.

TREK-1 and TREK-2 co-immunoprecipitate in Xenopus oocytes

Wild type and tagged TREK channels were coexpressed in *Xenopus* oocytes in different combinations. Solubilized membrane preparation from oocytes expressing TREK-1-V5+TREK-2-FLAG and TREK-1+TREK-2-FLAG showed similar signal on Western blot when probed with anti-FLAG Ab. (Fig. 8A). The specific signal at 72 kDa (marked by an arrow) was missing in the sample from TREK-1-V5+TREK-2 injected oocytes (while non-specific bands were apparent at higher and lower molecular weight regions). After immunoprecipitation of the solubized samples by the V5 immunaffinity resin only the preparation from the TREK-1-V5+ TREK-2-FLAG expressing oocytes showed FLAG-immunorectivity indicating the assembly of the two tagged subunits Fig. 8B). The blot shown is representative of 3 independent experiments.

TREK-1 and TREK-2 form functional heterodimers in HEK293T cells

In addition to *Xenopus* oocytes, heterodimerization of TREK-1 and TREK-2 subunits has also been demonstrated in a mammalian cell line, in HEK293T cells. For the verification of heterodimer formation, a similar pharmacological approach was used as in the case of the oocytes (illustrated in Fig. 2).

HEK293T cells expressing TREK-1, TREK-2 or the TREK-1-T2A-TREK construct (which leads to equimolar formation of TREK-1 and TREK-2 subunits) were used for the experiments. In contrast to the experiments in oocytes, the pH was only decreased from the physiological 7.4 by one pH unit, to 6.4. After EC acidification, 30 μM RR was added to medium. The effect of these manipulations on the TREK current were plotted against each other (Fig. 9). The data point averages of the TREK-1 and TREK-2 homodimers were connected as in Fig. 2.

In good accordance with the literature data and our previous experiments, TREK-1 was inhibited by EC acidification (37.4±5.9% inhibition, n=5), while TREK-2 was activated by the decrease in EC pH (current increased by 44.3±8.1%, n=4). TREK-1 was RR insensitive (1.1±7.1% activation, n=5) and TREK-2 was potently inhibited by the dye (75.9%±2.9% inhibiton, n=4). The pH and RR sensitivity of the TREK current resulting from expression of the TREK-1-T2A-TREK-2 construct deviated from the line connecting the homodimers (in a matter similar to the oocytes in Fig. 2.B.). These data indicate that TREK-1 and TREK-2 subunits also form functional heterodimers when expressed in mammalian cells.

TREK-1 and TREK-2 subunits assemble into heterodimeric channels in DRG neurons

Expression of both TREK-1 and TREK-2 subunits in the neurons of the dorsal root ganglia has been previously described by different groups (27-29). Based on this data we decided to investigate whether TREK-1/TREK-2 heterodimers are present in these neurons. In native tissues, alternative translation initiation can not be ruled out, leading to different variants of TREK-1 and TREK-2 subunits. Thus distinct unitary conductance levels may correspond to the heterodimers of different subunit composition, making the identification of heterodimer formation difficult on the basis of conductance. Therefore, we applied a pharmacological approach in single channel measurements.

Based on our results on outside-out membrane patches from *Xenopus* oocytes, sensitivity to spadin can be used to recognize a potassium channel as a TREK-1 homodimer or a TREK-1/TREK-2 heterodimer. After the recovery of the current from the inhibition by spadin, RR can be used for the identification of the channel. If the channel is RR sensitive, then the channel is a TREK-1/TREK-2 heterodimer, if not, then it is a TREK-1 homodimer.

Outside-out membrane patches were excised from DRG neurons. Potassium channel activity was detected in 16 out of 25 membrane patches. Only patches containing 1 or 2 channels were analysed. The effects of spadin (1 μM) and RR (30 μM) on channel activity were measured and plotted against each other (See Fig 10.A.). In 16 membrane patches, 21 distinct potassium channels were identified. Four channels were found to be resistant to both RR and spadin. Eight channels were spadin resistant, but potently inhibited by RR (for representative recording see Fig. 10.B.). Nine channels were sensitive to both spadin and RR (Fig. 10.C.). This inhibitory profile indicates that these potassium channels found in *DRG neurons* are formed by the heterodimeric assembly of TREK-1 and TREK-2 subunits. Heterodimeric assembly was thus confirmed in a native tissue.

Discussion

TREK channels are known to participate in diverse physiological processes, such as nociception and thermoreception (30), relaxation of visceral and vascular smooth muscle cells (31) and regulation of hormone secretion (32). They were also reported to have potential therapeutic importance in different disease states, e.g. clinical depression (33) and prevention of post ischemic brain damage (34).

In this report, using a pharmacological approach combined with measurements at the single channel level, we demonstrate heteromerization of TREK-1 and TREK-2 subunits in different expression systems (*Xenopus* oocytes, HEK293T cells) and also in native cells (in DRG neurons).

We have previously obtained evidence that functional channels are formed when two identical (TREK-2/TREK-2) subunits are concatenated. The current of this tandem channel was indistinguishable from the naturally assembled TREK-2 homodimers. In the present study we have experimentally confirmed, by mutating a pore domain in only one of the subunits, that the assembly of the joined subunits is highly preferred over the intermolecular random dimerization. In order to characterize the functionality and properties of TREK-1/TREK-2 channel we created a model; a concatenated construct in which the two different subunits were covalently linked together and thereby forced to heterodimerize. The tandem TREK-1/TREK-2 turned out to be functional; its acid sensitivity was similar to that of the TREK-1 homodimer and it was moderately inhibited by RR. The reduced RR-sensitivity is in good accordance with our previous report, in which mutation of the RR interacting amino acid (D135) in one of the TREK-2 subunits converted the TREK-2/TREK-2 tandem to be moderately RR sensitive (20). Based on this asymmetrically inherited pharmacological profile the tandem channel could be distinguished from the mixture of homodimers. Coexpression of TREK-1 and TREK-2 subunits leads to a current which has a different pH and RR sensitvity than expected from a linear combination of TREK-1 and TREK-2 currents. This can only be explained by spontaneous formation of functional TREK-1/TREK-2 heterodimers from the individual subunits. Interaction of the two subunits was confirmed by co-immunoprecipitation of tagged TREK-1 and TREK-2 subunits in *Xenopus* oocytes. Heterodimerization also occurred in mammalian cells (HEK293T), ruling out the possibility that TREK-1/TREK-2 only heterodimerize in the amphibian system.

TREK-1 and TREK-2 channels have different single channel conductances. Differentiating the two channels on the single channel level is complicated by the fact that both channels have multiple isoforms due to alternative translation initiation which possess different conductance levels (24,26). To advance our study of the heteromerization of TREK-1 and TREK-2 subunits, we eliminated the multiple conductance levels arising from alternative translation variants by creating mutant versions of the channels (TREK-1-L, TREK-2-S and TREK-2-S/TREK-1-L tandem) with single translation initiation site. As expected, the mutant channels had a pH and RR sensitivity similar to their wild type counterparts and also formed functional heterodimers.

When expressed in *Xenopus* oocytes, each mutant channel (TREK-1-L and TREK-2-S) had one distinct single channel conductance level in excised inside-out membrane patches. The tandem construct had an intermediate conductance level compared to the two homodimers, thus the three mutants could be distinguished on the basis of their single channel conductance. In oocytes coexpressing TREK-1-L and TREK-2-S subunits, we recorded single potassium channels with conductances corresponding to the TREK-1-L homodimer, the TREK-2-S homodimer and channels with an intermediate conductance similar to the tandem channel. The existence of this intermediate conductance channel can be explained by the formation of functional TREK-1-L/TREK-2-S heterodimers, thus demonstrating the heteromerization of TREK-1 and TREK-2 subunits also on the single channel level.

The effect of RR, EC acidification and the sortilin-derived neuropeptide spadin on single TREK channels was examined in outside-out membrane patches excised from *Xenopus* oocytes. EC acidification influenced single channel activity similarly to its effect on the macroscopic TREK currents. Acidification inhibited the activity of TREK-1 and tandem channels and augmented TREK-2 channel activity by decreasing or increasing the open probability of the channels, respectively. The degree of inhibition of channel activity by RR was also similar to the effect of RR on macroscopic TREK currents. TREK-1 was RR insensitive, while TREK-2 was potently inhibited by the dye. The tandem channel was moderately inhibited by RR. The decrease of channel activity by RR was due to a decrease in the open probability of TREK-2 and tandem channels. Application of RR also leads to a moderate, statistically not significant decrease of the unitary TREK-2 current.

In good accordance with the previous reports, TREK-1 was potently inhibited by spadin, while TREK-2 was not affected. The peptide inhibited the tandem channel, the degree of the effect was similar to that observed in the case of the TREK-1 homodimer. Inhibition of TREK-1 and tandem channel activity was the consequence of the decreased open probability. Spadin has been described as a selective TREK-1 inhibitor (TREK-2, TRAAK, TRESK and TASK-1 have all been described to be insensitive to spadin). We have demonstrated that the TREK-1/TREK-2 heterodimer is also a target of the peptide. The spadin interacting site has not been identified, but our results indicate that one TREK-1 subunit is sufficient to confer sensitivity to the peptide. Accordingly, spadin is a promising candidate for testing or confirming experimental results in which TREK-1 is suspected as a heteromeric partner (15).

The TASK-1/TASK-3 heterodimer has been identified in native cells based on its different inhibitory profile from the homomeric TASK-1 and TASK-3 channels (7-9). Based on our results, the TREK-1/TREK-2 heterodimer can be differentiated from other K_{2P} channels based on its unique inhibitory profile. Application of spadin can be used to identify the current of TREK-1 or TREK-1/TREK-2 heterodimer. The spadin-sensitive current can be further differentiated by RR; the insensitive component reflects TREK-1 homodimer, while the spadin-sensitive current with intermediate RR sensitivity can be identified as TREK-1/TREK-2.

TREK-1 and TREK-2 subunits are widely expressed in both the central nervous system and in peripheral tissues. Overlapping expression of the two subunits has been reported in the striatum and in the hippocampus (for review see (35)). Native channels with properties corresponding to TREK-1 and TREK-2 and a TREK-like channel (with properties different from TREK-1, TREK-2 and TRAAK) have been described in magnocellular neurosecretory cells of the supraoptic nucleus (36). The expression of both subunits has also been detected in the peripheral (27-29) superior cervical

ganglia (37). Co-expression of TREK-1 and TREK-2 subunits has also been described in non-neuronal cells, for example in pulmonary vascular smooth muscle cells (31).

Heterodimerization of TREK-1 and TREK-2 subunits has also been examined in neurons of dorsal root ganglia. We excised outside-out membrane patches from cultured DRG neurons and examined the effect of spadin and RR on the channel activity. We could group the channels into three distinct groups: spadin- and RR-resistant channels, spadin-resistant and RR-sensitive channels and a spadin- and RR-sensitive group. The spadin- and RR-insensitive currents may correspond to TRESK or TASK-1 or other K^+ channels. The spadin resistant and RR-sensitive ones may correspond to TREK-2, TRAAK or TASK-3. Exact identification of these channels, however, was beyond the scope of the present study. The channels of the third group were inhibited by both spadin and RR. Sensitivity to the specific peptide inhibitor spadin suggests that these channels contained TREK-1 subunit. Sensitivity of the same channel to RR clearly indicated the presence of another, RR-sensitive subunit in the channel complex, i.e. the formation of the heterodimer.

Changes in EC pH regulate the membrane potential and excitability of pulmonary vascular smooth muscle cells and somatosensory neurons. These cells express both TREK-1 and TREK-2 subunits. The TREK-1/TREK-2 heterodimer and the TREK-1 homodimer have a similar sensitivity to EC acidification, but the heterodimeric channel has a larger conductance than the TREK-1 homodimer. Assembly of identical number of heterodimers instead of TREK-1 homodimers may lead to a larger background potassium current. A change in the ratio of the heterodimers compared to TREK-1 homodimers can regulate the amplitude of the background potassium conductance, thus controlling the excitability of the cell without changing the overall sensitivity of the current to EC pH. The TREK-1/TREK-2 heterodimer can thus contribute to the control of DRG neuron excitability.

Spadin is a byproduct of the maturation of the sortilin receptor. In mouse models of depression, spadin had an effect similar to fluoxetine, an antidepressant used in the treatment of clinical depression. The antidepressant effects of spadin were apparent after 5-6 days of application, while the effect of conventional antidepressants only manifest after 2-3 weeks of treatment. Therefore, spadin has been considered as an endogenous antidepressant (18). According to the present results the peptide might well be an endogenous regulator of TREK-1/TREK-2 heterodimer activity. In neurons, inhibition of TREK-1/TREK-2 heterodimer by spadin can lead to membrane depolarization and increased transmitter release. We have demonstrated that TREK-1 and TREK-2 heterodimerize in neurons of the peripheral nervous system, however, heterodimer formation may also happen in the central nervous system. In this case inhibition of the heterodimeric channel may contribute to the antidepressant effect of spadin.

Acknowledgements: This work was supported by the Hungarian National Research Fund (OTKA K108496). The skillful technical assistance of Irén Veres, Alice Dobolyi and Péter Bozsaki is acknowledged.

Conflict of interest: None declared.

Author Contributions: ML designed and performed experiments, analyzed data and wrote the paper. GC and PE designed experiments, analyzed data and wrote the paper.

References:

1. Coetzee, W. A., Amarillo, Y., Chiu, J., Chow, A., Lau, D., McCormack, T., Moreno, H., Nadal, M. S., Ozaita, A., Pountney, D., Saganich, M., Vega-Saenz de Miera, E., and Rudy, B. (1999) Molecular diversity of K+ channels. *Ann N Y Acad Sci* **868**, 233-285
2. Wissinger, B., Schaich, S., Baumann, B., Bonin, M., Jagle, H., Friedburg, C., Varsányi, B., Hoyng, C. B., Dollfus, H., Heckenlively, J. R., Rosenberg, T., Rudolph, G., Kellner, U., Salati, R., Plomp, A., De Baere, E., Andrassi-Darida, M., Sauer, A., Wolf, C., Zobor, D., Bernd, A., Leroy, B. P., Enyedi, P., Cremers, F. P., Lorenz, B., Zrenner, E., and Kohl, S. (2011) Large deletions of the KCNV2 gene are common in patients with cone dystrophy with supernormal rod response. *Hum Mutat* **32**, 1398-1406
3. Smith, K. E., Wilkie, S. E., Tebbs-Warner, J. T., Jarvis, B. J., Gallasch, L., Stocker, M., and Hunt, D. M. (2012) Functional analysis of missense mutations in Kv8.2 causing cone dystrophy with supernormal rod electroretinogram. *J Biol Chem* **287**, 43972-43983
4. Gilling, M., Rasmussen, H. B., Calloe, K., Sequeira, A. F., Baretto, M., Oliveira, G., Almeida, J., Lauritsen, M. B., Ullmann, R., Boonen, S. E., Brondum-Nielsen, K., Kalscheuer, V. M., Tumer, Z., Vicente, A. M., Schmitt, N., and Tommerup, N. (2013) Dysfunction of the Heteromeric KV7.3/KV7.5 Potassium Channel is Associated with Autism Spectrum Disorders. *Front Genet* **4**, 54
5. Enyedi, P., and Czirják, G. (2010) Molecular background of leak K+ currents: two-pore domain potassium channels. *Physiol Rev* **90**, 559-605
6. Czirják, G., and Enyedi, P. (2002) Formation of functional heterodimers between the TASK-1 and TASK-3 two-pore domain potassium channel subunits. *J Biol Chem* **277**, 5426-5432
7. Berg, A. P., Talley, E. M., Manger, J. P., and Bayliss, D. A. (2004) Motoneurons express heteromeric TWIK-related acid-sensitive K+ (TASK) channels containing TASK-1 (KCNK3) and TASK-3 (KCNK9) subunits. *J Neurosci* **24**, 6693-6702
8. Kang, D., Han, J., Talley, E. M., Bayliss, D. A., and Kim, D. (2004) Functional expression of TASK-1/TASK-3 heteromers in cerebellar granule cells. *J Physiol* **554**, 64-77
9. Kim, D., Cavanaugh, E. J., Kim, I., and Carroll, J. L. (2009) Heteromeric TASK-1/TASK-3 is the major oxygen-sensitive background K+ channel in rat carotid body glomus cells. *J Physiol* **587**, 2963-2975
10. Larkman, P. M., and Perkins, E. M. (2005) A TASK-like pH- and amine-sensitive 'leak' K+ conductance regulates neonatal rat facial motoneuron excitability in vitro. *Eur J Neurosci* **21**, 679-691
11. Meuth, S. G., Aller, M. I., Munsch, T., Schuhmacher, T., Seidenbecher, T., Meuth, P., Kleinschnitz, C., Pape, H. C., Wiendl, H., Wisden, W., and Budde, T. (2006) The contribution of TWIK-related acid-sensitive K+-containing channels to the function of dorsal lateral geniculate thalamocortical relay neurons. *Mol Pharmacol* **69**, 1468-1476
12. Torborg, C. L., Berg, A. P., Jeffries, B. W., Bayliss, D. A., and McBain, C. J. (2006) TASK-like conductances are present within hippocampal CA1 stratum oriens interneuron subpopulations. *J Neurosci* **26**, 7362-7367
13. Blin, S., Chatelain, F. C., Feliciangeli, S., Kang, D., Lesage, F., and Bichet, D. (2014) Tandem pore domain halothane-inhibited K+ channel subunits THIK1 and THIK2 assemble and form active channels. *J Biol Chem* **289**, 28202-28212
14. Plant, L. D., Zuniga, L., Araki, D., Marks, J. D., and Goldstein, S. A. (2012) SUMOylation silences heterodimeric TASK potassium channels containing K2P1 subunits in cerebellar granule neurons. *Sci Signal* **5**, ra84

15. Hwang, E. M., Kim, E., Yarishkin, O., Woo, D. H., Han, K. S., Park, N., Bae, Y., Woo, J., Kim, D., Park, M., Lee, C. J., and Park, J. Y. (2014) A disulphide-linked heterodimer of TWIK-1 and TREK-1 mediates passive conductance in astrocytes. *Nat Commun* **5**, 3227
16. Bagriantsev, S. N., Peyronnet, R., Clark, K. A., Honore, E., and Minor, D. L., Jr. (2011) Multiple modalities converge on a common gate to control K2P channel function. *EMBO J* **30**, 3594-3606
17. Sandoz, G., Douguet, D., Chatelain, F., Lazdunski, M., and Lesage, F. (2009) Extracellular acidification exerts opposite actions on TREK1 and TREK2 potassium channels via a single conserved histidine residue. *Proc Natl Acad Sci U S A* **106**, 14628-14633
18. Mazella, J., Petrault, O., Lucas, G., Deval, E., Beraud-Dufour, S., Gandin, C., El-Yacoubi, M., Widmann, C., Guyon, A., Chevet, E., Taouji, S., Conductier, G., Corinus, A., Coppola, T., Gobbi, G., Nahon, J. L., Heurteaux, C., and Borsotto, M. (2010) Spadin, a sortilin-derived peptide, targeting rodent TREK-1 channels: a new concept in the antidepressant drug design. *PLoS Biol* **8**, e1000355
19. Moha Ou Maati, H., Veyssiere, J., Labbal, F., Coppola, T., Gandin, C., Widmann, C., Mazella, J., Heurteaux, C., and Borsotto, M. (2012) Spadin as a new antidepressant: absence of TREK-1-related side effects. *Neuropharmacology* **62**, 278-288
20. Braun, G., Lengyel, M., Enyedi, P., and Czirják, G. (2015) Differential sensitivity of TREK-1, TREK-2 and TRAAK background potassium channels to the polycationic dye ruthenium red. *British Journal of Pharmacology* **172**, 1728-1738
21. Czirják, G., and Enyedi, P. (2006) Zinc and mercuric ions distinguish TRESK from the other two-pore-domain K+ channels. *Mol Pharmacol* **69**, 1024-1032
22. Szymczak, A. L., Workman, C. J., Wang, Y., Vignali, K. M., Dilioglou, S., Vanin, E. F., and Vignali, D. A. (2004) Correction of multi-gene deficiency in vivo using a single 'self-cleaving' 2A peptide-based retroviral vector. *Nat Biotechnol* **22**, 589-594
23. Tóth, J. T., Gulyás, G., Tóth, D. J., Balla, A., Hammond, G. R., Hunyady, L., Balla, T., and Várnai, P. (2016) BRET-monitoring of the dynamic changes of inositol lipid pools in living cells reveals a PKC-dependent PtdIns4P increase upon EGF and M3 receptor activation. *Biochim Biophys Acta* **1861**, 177-187
24. Thomas, D., Plant, L. D., Wilkens, C. M., McCrossan, Z. A., and Goldstein, S. A. (2008) Alternative translation initiation in rat brain yields K2P2.1 potassium channels permeable to sodium. *Neuron* **58**, 859-870
25. Czirják, G., Tóth, Z. E., and Enyedi, P. (2004) The two-pore domain K+ channel, TRESK, is activated by the cytoplasmic calcium signal through calcineurin. *J Biol Chem* **279**, 18550-18558
26. Simkin, D., Cavanaugh, E. J., and Kim, D. (2008) Control of the single channel conductance of K2P10.1 (TREK-2) by the amino-terminus: role of alternative translation initiation. *J Physiol* **586**, 5651-5663
27. Kang, D., and Kim, D. (2006) TREK-2 (K2P10.1) and TRESK (K2P18.1) are major background K+ channels in dorsal root ganglion neurons. *Am J Physiol Cell Physiol* **291**, C138-146
28. Talley, E. M., Solorzano, G., Lei, Q., Kim, D., and Bayliss, D. A. (2001) Cns distribution of members of the two-pore-domain (KCNK) potassium channel family. *J Neurosci* **21**, 7491-7505
29. Usoskin, D., Furlan, A., Islam, S., Abdo, H., Lonnerberg, P., Lou, D., Hjerling-Leffler, J., Haeggstrom, J., Kharchenko, O., Kharchenko, P. V., Linnarsson, S., and Ernfors, P. (2015) Unbiased classification of sensory neuron types by large-scale single-cell RNA sequencing. *Nat Neurosci* **18**, 145-153
30. Noel, J., Zimmermann, K., Busserolles, J., Deval, E., Alloui, A., Diochot, S., Guy, N., Borsotto, M., Reeh, P., Eschalier, A., and Lazdunski, M. (2009) The mechano-activated K+ channels TRAAK and TREK-1 control both warm and cold perception. *EMBO J* **28**, 1308-1318

31. Koh, S. D., Monaghan, K., Sergeant, G. P., Ro, S., Walker, R. L., Sanders, K. M., and Horowitz, B. (2001) TREK-1 regulation by nitric oxide and cGMP-dependent protein kinase. An essential role in smooth muscle inhibitory neurotransmission. *J Biol Chem* **276**, 44338-44346
32. Enyeart, J. J., Xu, L., Danthi, S., and Enyeart, J. A. (2002) An ACTH- and ATP-regulated background K+ channel in adrenocortical cells is TREK-1. *J Biol Chem* **277**, 49186-49199
33. Heurteaux, C., Lucas, G., Guy, N., El Yacoubi, M., Thummler, S., Peng, X. D., Noble, F., Blondeau, N., Widmann, C., Borsotto, M., Gobbi, G., Vaugeois, J. M., Debonnel, G., and Lazdunski, M. (2006) Deletion of the background potassium channel TREK-1 results in a depression-resistant phenotype. *Nat Neurosci* **9**, 1134-1141
34. Heurteaux, C., Laigle, C., Blondeau, N., Jarretou, G., and Lazdunski, M. (2006) Alpha-linolenic acid and riluzole treatment confer cerebral protection and improve survival after focal brain ischemia. *Neuroscience* **137**, 241-251
35. Noel, J., Sandoz, G., and Lesage, F. (2011) Molecular regulations governing TREK and TRAAK channel functions. *Channels (Austin)* **5**, 402-409
36. Han, J., Gnatenco, C., Sladek, C. D., and Kim, D. (2003) Background and tandem-pore potassium channels in magnocellular neurosecretory cells of the rat supraoptic nucleus. *The Journal of Physiology* **546**, 625-639
37. Cadaveira-Mosquera, A., Perez, M., Reboreda, A., Rivas-Ramirez, P., Fernandez-Fernandez, D., and Lamas, J. A. (2012) Expression of K2P channels in sensory and motor neurons of the autonomic nervous system. *J Mol Neurosci* **48**, 86-96

Figure legends

Figure 1: Different inhibitory profiles of TREK-1, TREK-2 and the TREK-2/TREK-1 tandem channel.

TREK-1, TREK-2 and TREK-2/TREK-1 tandem channels were expressed in *Xenopus* oocytes. Oocytes were measured with the two electrode voltage clamp method 2-3 days after injection. Currents were measured at -100 mV. Holding potential was -75 mV. $[K^+]$ was switched from 2 mM to 40 mM, then back to 2 mM as shown above the graphs. Acidification of the bath solution and application of 30 μM RR are indicated by the horizontal bars above the recordings. The nonspecific leak current measured in 2 mM K^+ was subtracted from the currents. The currents were normalized to the value measured in 40 mM K^+. The average of multiple recordings was plotted, error bars indicate S.E.M.

A, TREK-1 is inhibited by extracellular acidification and is RR insensitive (n=10 oocytes).

B, TREK-2 is activated by extracellular acidification and is potently inhibited by RR (n=6 oocytes).

C, The TREK-2/TREK-1 tandem channel is inhibited by extracellular acidification and has an intermediate RR sensitivity (n=8 oocytes).

D, The sensitivity of TREK channels to extracellular acidification. TREK-1 (white circles) and the tandem channel (black diamonds) are inhibited (there was no significant difference between the degree of inhibition, p=0.34), while TREK-2 (grey triangles) is activated by lowering the extracellular pH. Averages of the groups are plotted as columns.

E, The sensitivity of TREK channels to RR. TREK-1 (white circles) is insensitive, while TREK-2 (grey triangles) is greatly inhibited by RR. The tandem channel (black diamonds) has an intermediate sensitivity. The degree of inhibition is significantly different between all three groups ($p<10^{-6}$). Averages of the groups are plotted as columns.

Figure 2.: TREK-1 and TREK-2 subunits form functional heterodimers in *Xenopus* oocytes.

A, *Xenopus* oocytes were injected with TREK-1 (circles), TREK-2 (triangles) or TREK-2/TREK-1 tandem (diamonds) cRNA. TREK currents were measured as described in Figure 1. The sensitivity of the currents to extracellular acidification and RR application were plotted against each other. Averages of the three groups (empty diamonds) are shown with error bars representing S.E.M. The straight line connects the averages of the groups expressing TREK-1 or TREK-2 homodimers, respectively.

B, *Xenopus* oocytes were injected with different ratios of TREK-1 and TREK-2 cRNA (squares). The pH and RR sensitivity of the expressed TREK currents were measured as in Figure 1 and plotted as in Figure 2A. The averages (with error bars) of the 3 groups and the straight line from Figure 2A are also displayed.

Figure 3.: Different single channel conductances of N-terminal mutant TREK channels

TREK-1-L, TREK-2-S and TREK-2-S/TREK-1-L tandem channels were expressed in *Xenopus* oocytes. Currents were recorded from inside-out membrane patches at a membrane potential of +60 mV. The pipette solution contained (in mM): 136 NaCl, 4 KCl, 5 EGTA and 10 HEPES (pH 7.4 adjusted with NaOH). Bath solution contained (in mM): 140 KCl, 5 EGTA and 10 HEPES (pH 7.1 adjusted with KOH). The charge carrier of the currents recorded was verified by K^+-free bath solution (140 NaCl, 5 EGTA and 10 HEPES, pH 7.1 adjusted with NaOH). Current traces displayed were filtered at 2 kHz.

A, Representative current recordings of inside-out membrane patches from *Xenopus* oocytes expressing TREK-1-L (top), TREK-2-S (middle) and TREK-2-S/TREK-1-L tandem (bottom) in a high $[K^+]$ bath solution at a membrane potential of +60 mV. No outward current was detected in K^+-free bath solution. Currents were recorded in high $[K^+]$ bath solution for 30-60 s.

B, All points histograms were created from recordings of TREK-1-L (top), TREK-2-S (middle) and TREK-2-S/TREK-1-L tandem (bottom). Unitary currents and single channel conductances were calculated from the amplitude histograms.

C, Single channel conductances of TREK-1-L (white circles, n=6 patches), TREK-2-S (grey triangles, n=7 patches) and TREK-2-S/TREK-1-L (black diamonds, n=8 patches) are displayed as a scatter plot. The averages of the three groups are plotted as columns. The difference between the conductance of all three groups was found to be statistically significant ($p<0.01$).

Figure 4.: Formation of TREK-1-L/TREK-2-S heterodimers

Xenopus oocytes were injected with different ratios of TREK-1-L and TREK-2-S cRNA. Currents were recorded from inside-out membrane patches as described in Figure 3. Unitary currents and single channel conductances were calculated from patches containing one channel and plotted in the function of injected RNA ratios. For comparision, the averages (± SD) of TREK-1, TREK-2 and TREK-2-S/TREK-1-L tandem channel unitary currents were also plotted.

Figure 5.: Effect of RR on single TREK channels

TREK-1-L, TREK-2-S and TREK-2-S/TREK-1-L tandem channels were expressed in *Xenopus* oocytes. Single channel currents were recorded in symmetrical 140 mM K^+ from outside-out membrane patches. Current traces displayed were filtered at 2 kHz.

A-C, Representative current recordings of outside-out membrane patches from *Xenopus* oocytes expressing TREK-1-L (A), TREK-2-S (B)and TREK-2-S/TREK-1-L tandem (C) at a membrane potential of -60 mV. Application of 30 μM RR is indicated by the horizontal bar on the recordings. The effect of RR was reversible. Channel activity (NP_o) was determined from 30-60 s of recording before, during and after application of RR.

D, Effect of 30 μM RR on channel activity of TREK-1-L (white circles, n=4 patches), TREK-2-S (grey triangles, n=7 patches) and TREK-2-S/TREK-1-L (black diamonds, n=4 patches) channels is displayed as a scatter plot. The averages of the three groups are plotted as columns. The difference between the effect of RR on the channel activity of all three groups was found to be statistically significant ($p<0.05$).

Figure 6.: Effect of extracellular acidification on single TREK channels

TREK-1-L, TREK-2-S and TREK-2-S/TREK-1-L tandem channels were expressed in *Xenopus* oocytes. Single channel currents were recorded in symmetrical 140 mM [K^+] from outside-out membrane patches. Current traces displayed were filtered at 2 kHz.

A-C, Representative current recordings of outside-out membrane patches from *Xenopus* oocytes expressing TREK-1-L (A), TREK-2-S (B) and TREK-2-S/TREK-1-L tandem (C) at a membrane potential of -60 mV. Acidification of the bath (pH 7.4 to pH 6.4) is indicated by the horizontal bar. The effect of the decrease in the extracellular pH was reversible by switching back the pH of the bath medium to pH 7.4. Channel activity (NP_o) was determined from 30-60 s of recording before, during and after acidification of the bath.

D, Effect of extracellular acidification on channel activity of TREK-1-L (white circles, n=5 patches), TREK-2-S (grey triangles, n=5 patches) and TREK-2-S/TREK-1-L (black diamonds, n=4 patches) channels is displayed as a scatter plot. The averages of the groups are plotted as columns. The difference between the effect of extracellular acidification on the channel activity of TREK-2-S compared to TREK-1-L and TREK-2-S/TREK-1-L was found to be statistically significant ($p<10^{-3}$). The difference between the effect of extracellular acidification on the channel activity of TREK-1-L and TREK-2-S/TREK-1-L was not significant ($p=0.94$).

Figure 7.: Effect of spadin on single TREK channels

TREK-1-L, TREK-2-S and TREK-2-S/TREK-1-L tandem channels were expressed in *Xenopus* oocytes. Single channel currents were recorded in symmetrical 140 mM [K^+] from outside-out membrane patches. Current traces displayed were filtered at 2 kHz.

A-C, Representative current recordings of outside-out membrane patches from *Xenopus* oocytes expressing TREK-1-L (A), TREK-2-S (B) and TREK-2-S/TREK-1-L tandem (C) at a membrane potential of -60 mV. Application of spadin (1 μM) is indicated by the horizontal bar. The effect of spadin was reversible. Channel activity (NP_o) was determined from 30-60 s of recording before, during and after application of spadin.

D, Effect of spadin on channel activity of TREK-1-L (white circles, n=4 patches), TREK-2-S (grey triangles, n=4 patches) and TREK-2-S/TREK-1-L (black diamonds, n=5 patches) channels is displayed as a scatter plot. The averages of the groups are plotted as columns. The difference between the effect of spadin on the

channel activity of TREK-2-S compared to TREK-1-L and TREK-2-S/TREK-1-L was found to be statistically significant ($p<0.05$). The difference between the effect of spadin on the channel activity of TREK-1-L and TREK-2-S/TREK-1-L was not significant ($p=0.38$).

Figure 8.: Co-immunoprecipitation of TREK-1 and TREK-2 subunits

Xenopus oocytes were coinjected with cRNA of TREK-1 and TREK-2 channel constructs, in different combinations of wild type or epitope tagged forms, as indicated.

A, Total membrane lysates were prepared, solubilized and subjected to SDS-PAGE. Size fractionated proteins were transfered to nitrocellulose membrane, the blots were probed with monoclonal anti-FLAG Ab. and visualized by HRP conjugated anti mouse Ab. The arrow marks the specific TREK-2-FLAG immunoreactivity.

B, Co-immunoprecipitation was performed on solubilized membrane preparations using beads to which polyclonal anti-V5 antibody was bound. The affinity purified proteins were analyzed as described at Panel A. The blot shown is representative of 3 independent experiments.

Figure 9.: TREK-1 and TREK-2 form heterodimers in HEK293T cells

HEK293T cells were transfected with plasmids coding TREK-1 (circles), TREK-2 (triangles) or TREK-1-T2A-TREK-2 (diamonds). The sensitivity of the currents to extracellular acidification (pH 7.4 to pH 6.4) and RR application (30 μM) were plotted against each other. Averages of the three groups (empty diamonds) are shown with error bars representing S.E.M. The straight line connects the averages of the groups expressing TREK-1 or TREK-2 homodimers, respectively.

Figure 10.: TREK-1 and TREK-2 subunits heterodimerize in dorsal root ganglion neurons

Membrane patches were excised from DRG neurons. Single channel currents were recorded in symmetrical 140 mM [K^+] in the outside-out configuration. The effect of spadin (1 μM) and RR (30 μM) application were determined at a membrane potential of -60 mV. Application of spadin and RR is indicated by the horizontal bars. Channel activity (NP_o) was determined from 30-60 s of recording before, during and after application of spadin and RR. Current traces displayed were filtered at 2 kHz. Channels resistant to both spadin and RR (n=4) were not plotted.

A, The effect of spadin (1 μM) and RR (30 μM) on channel activity were plotted against each other. Triangles represent RR-sensitive, but spadin resistant channels. TREK-1/TREK-2 heterodimers are marked by the circles.

B, Representative current recording of a patch containing two RR-sensitive and spadin-resistant channels.

C, Representative current recording of a patch containing a channel inhibited by RR and spadin, (regarded as a TREK-1/TREK-2 heterodimer).

Figure 1.

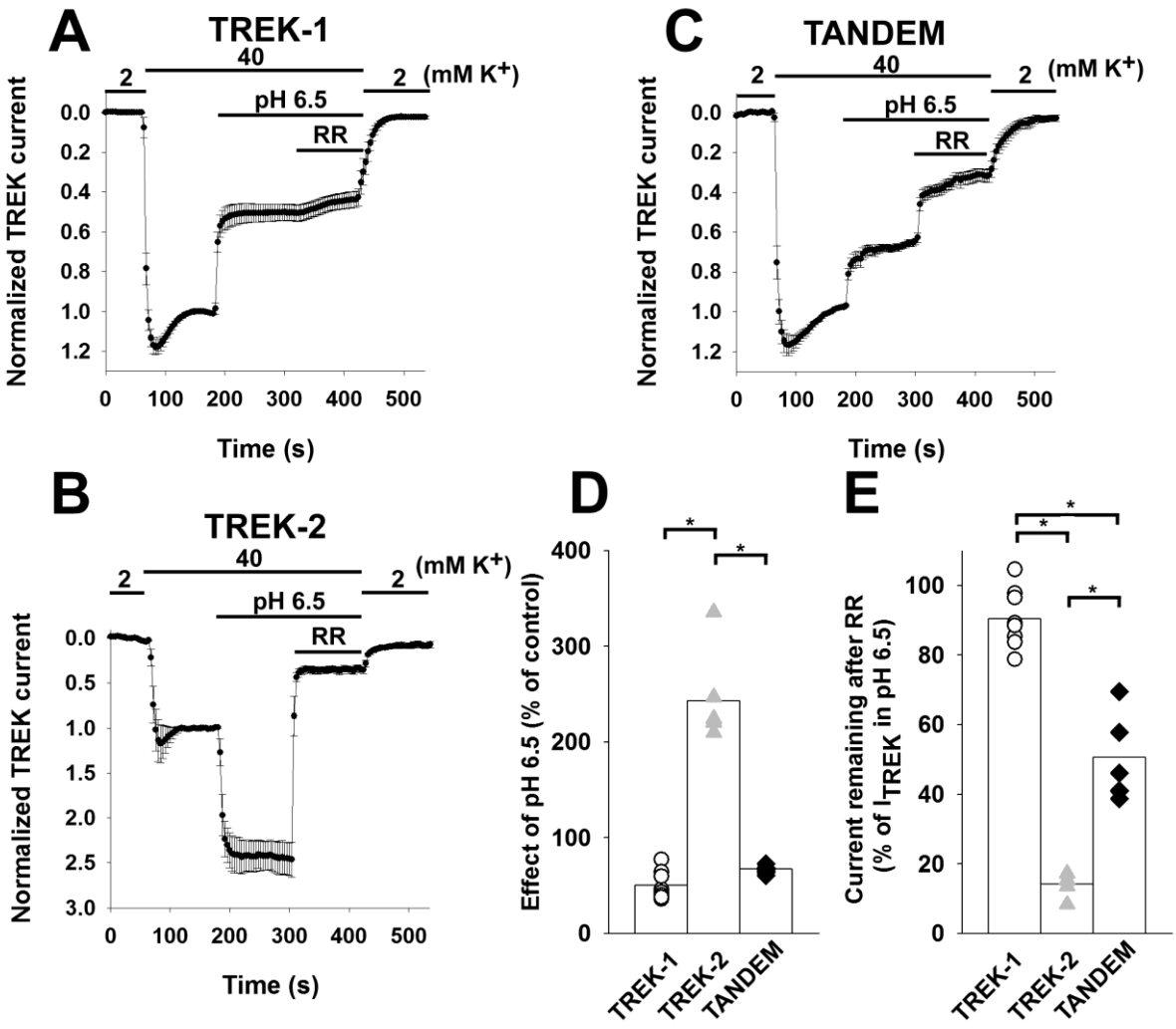

Figure 2.

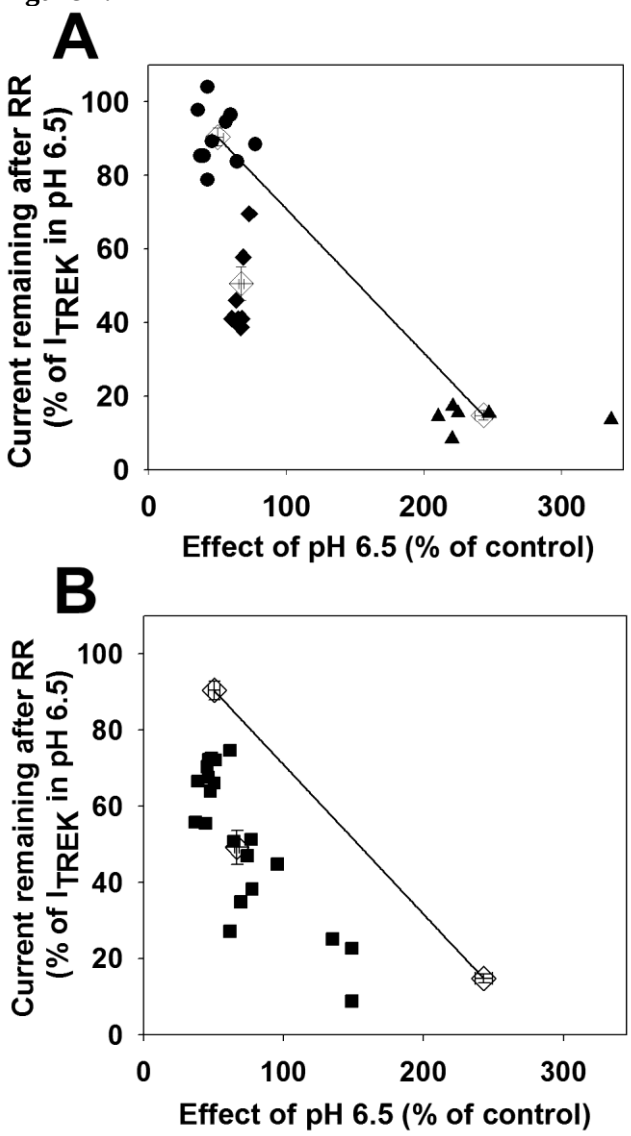

Figure 3.

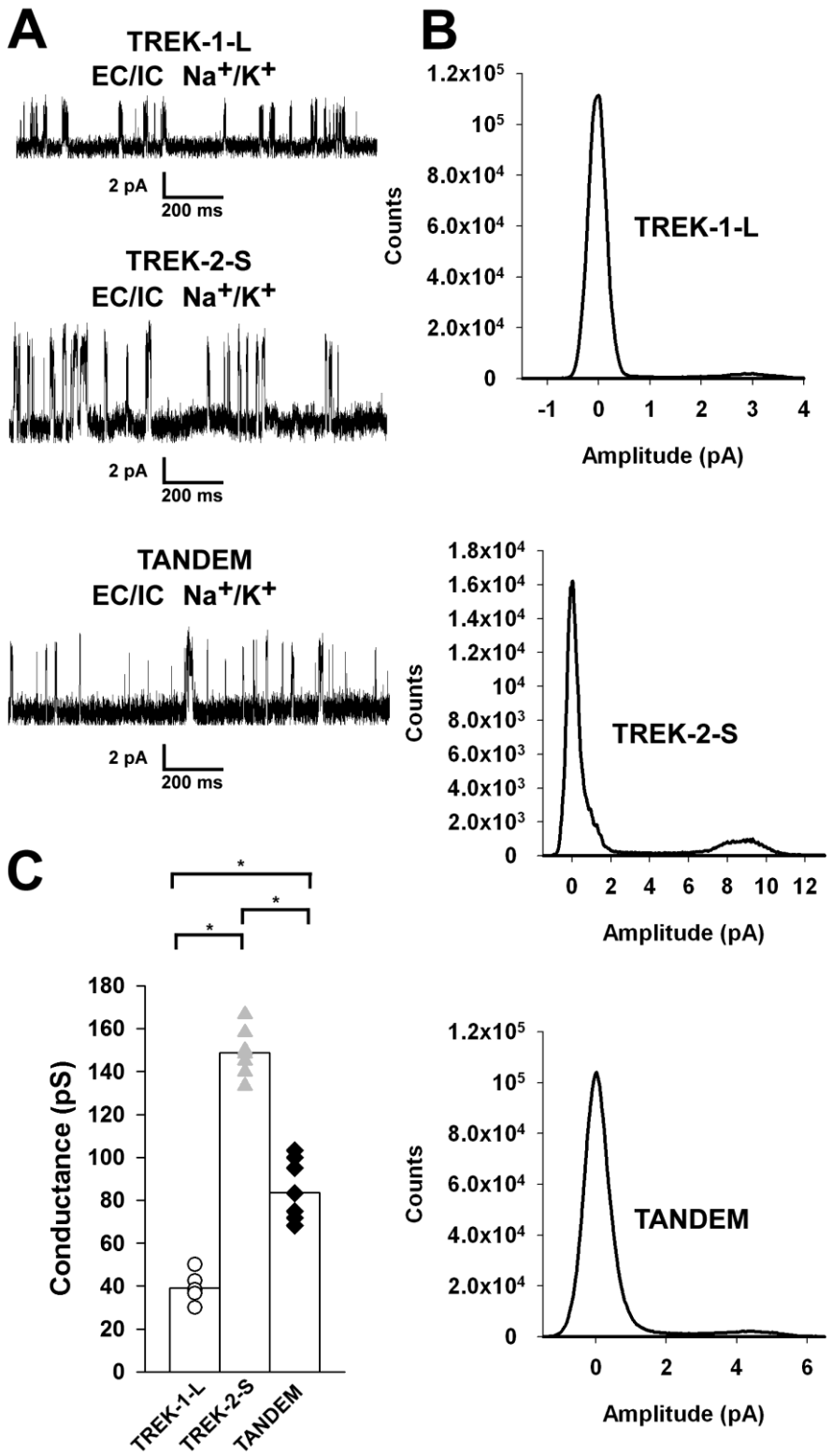

Figure 4.

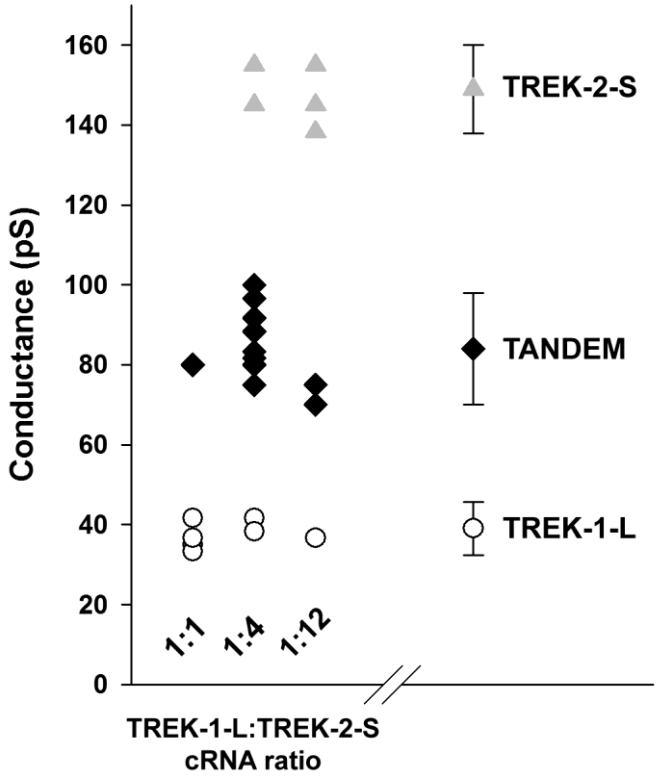

Figure 5.

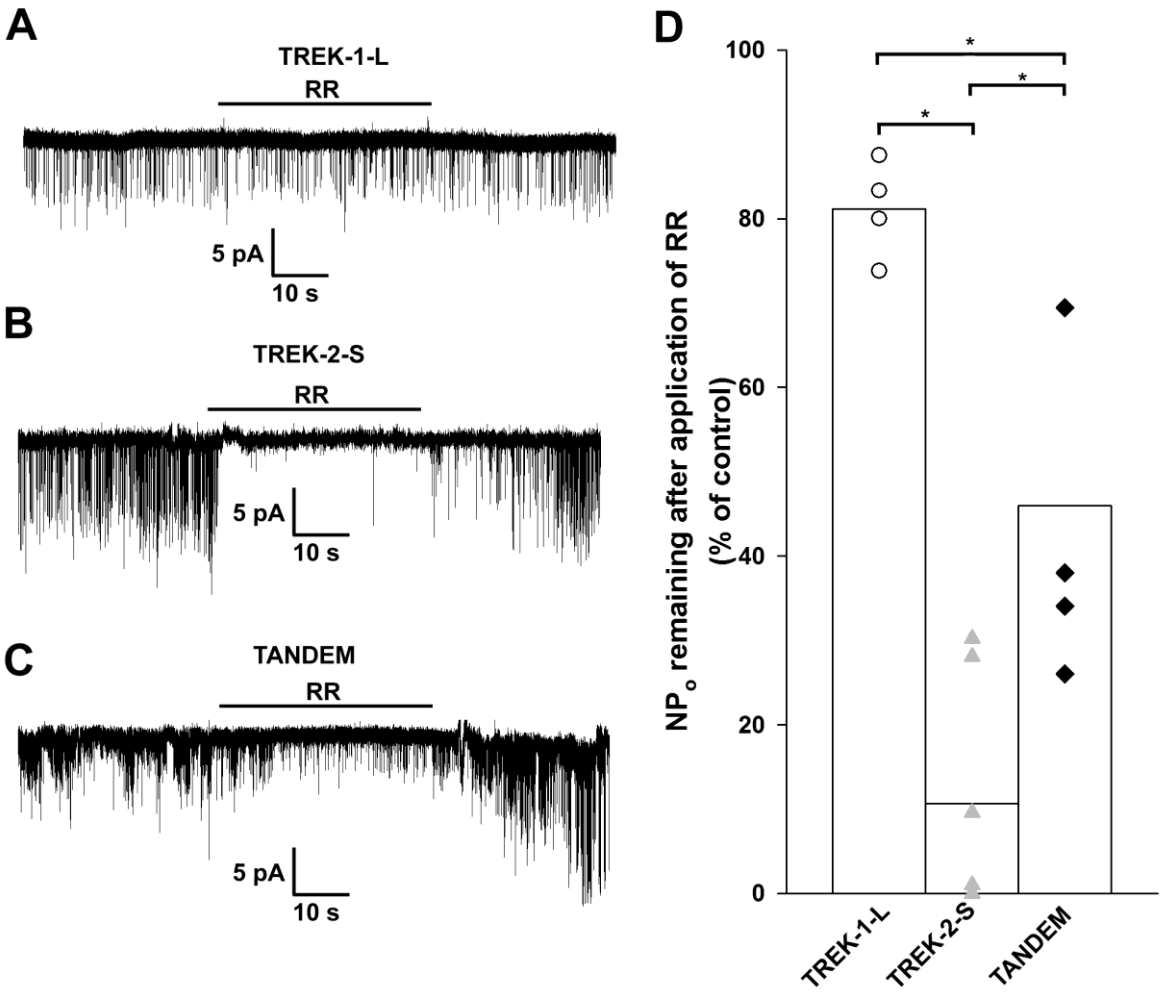

Figure 6.

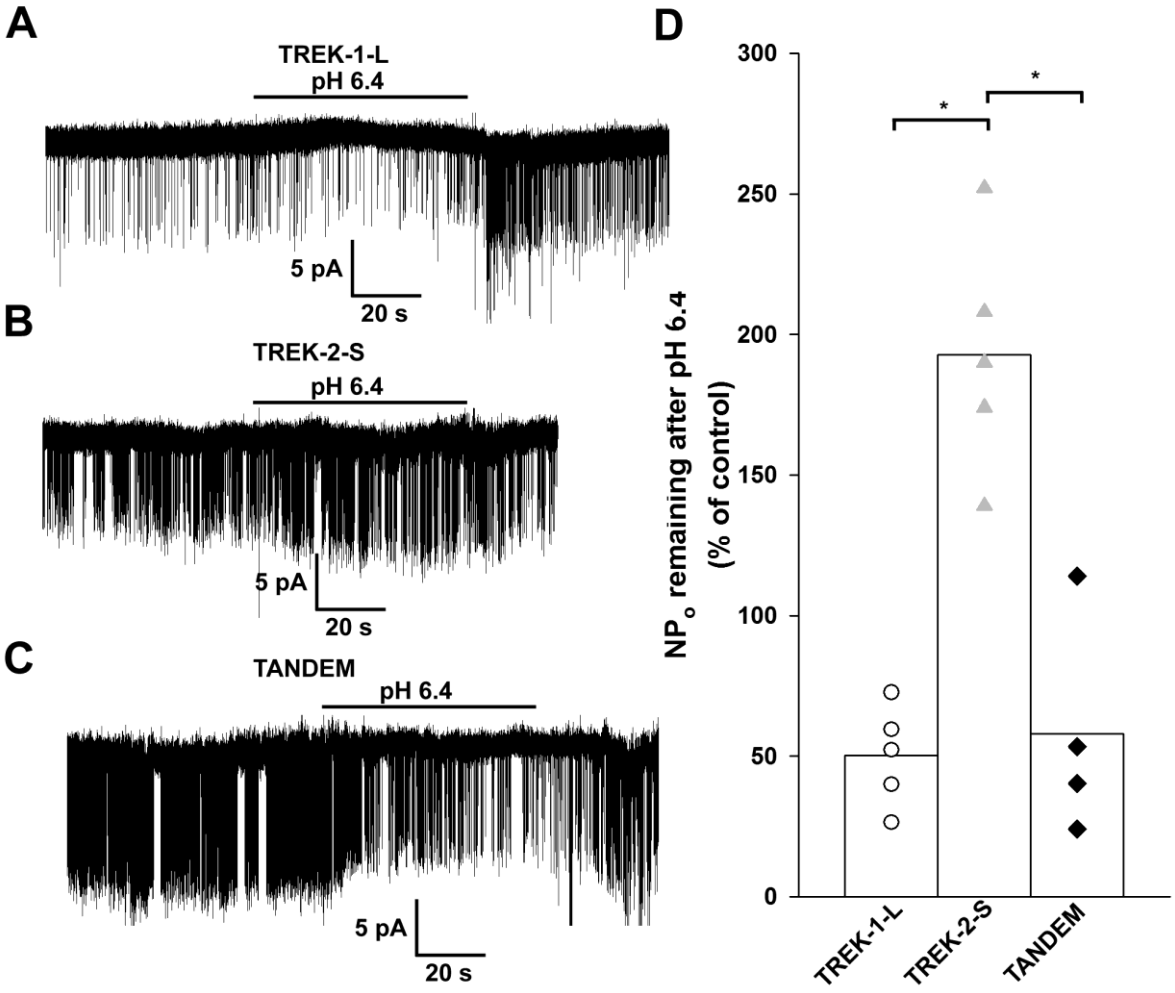

Figure 7.

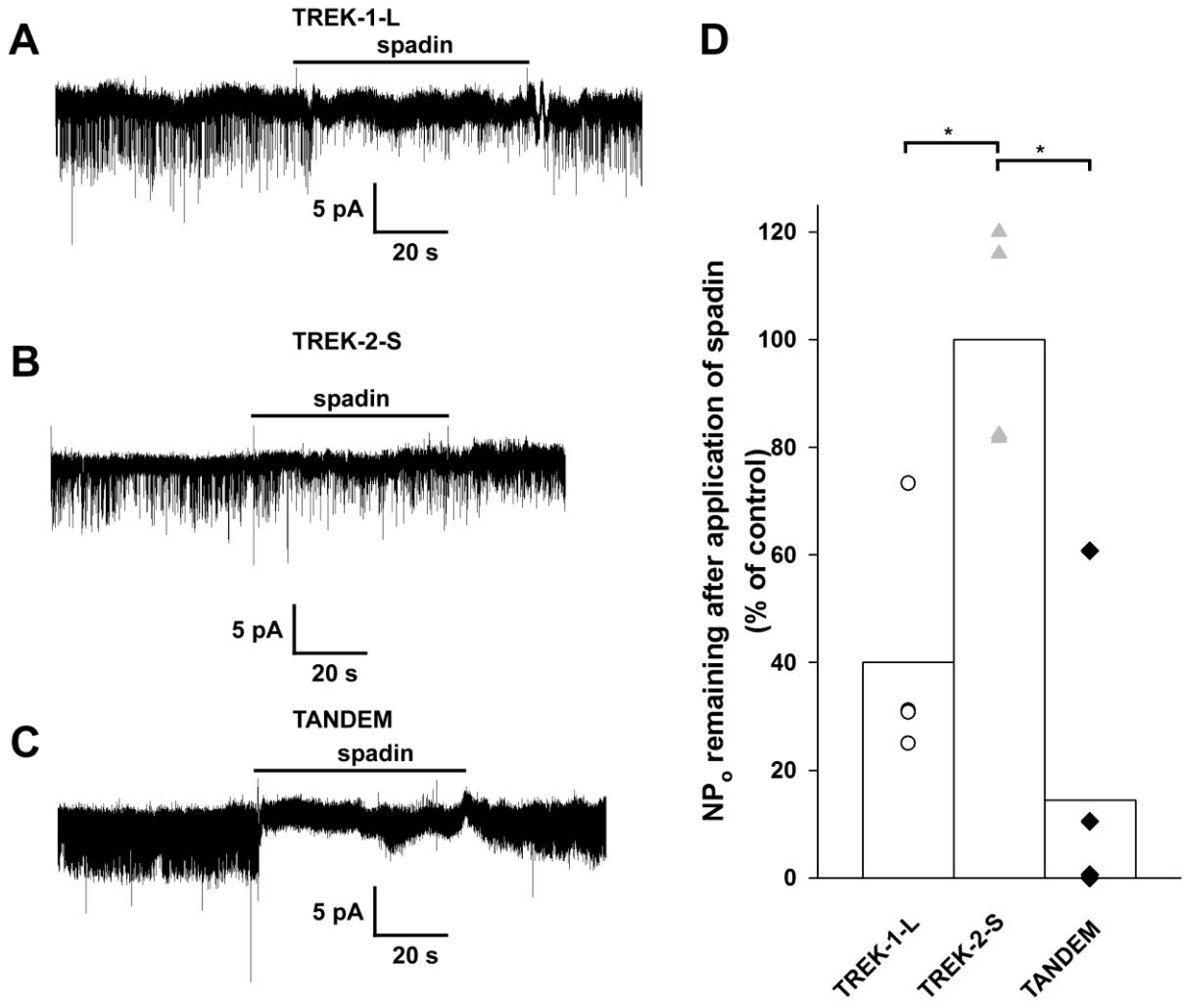

Figure 8.

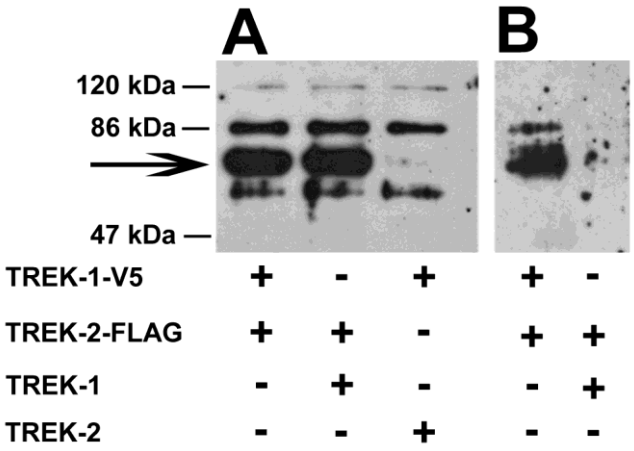

Figure 9.

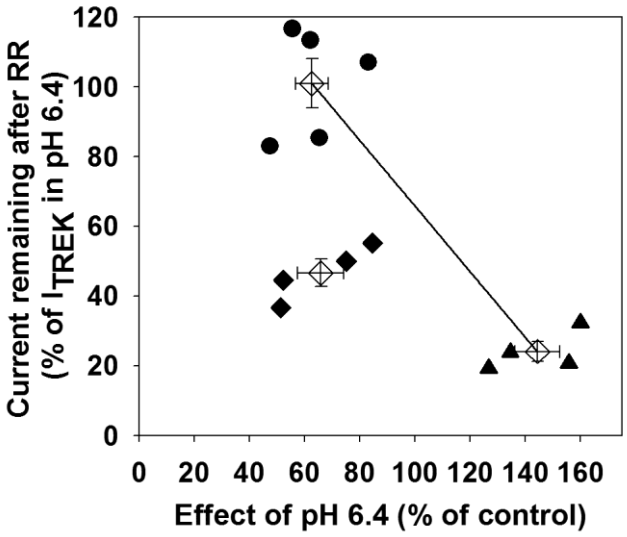

Figure 10.

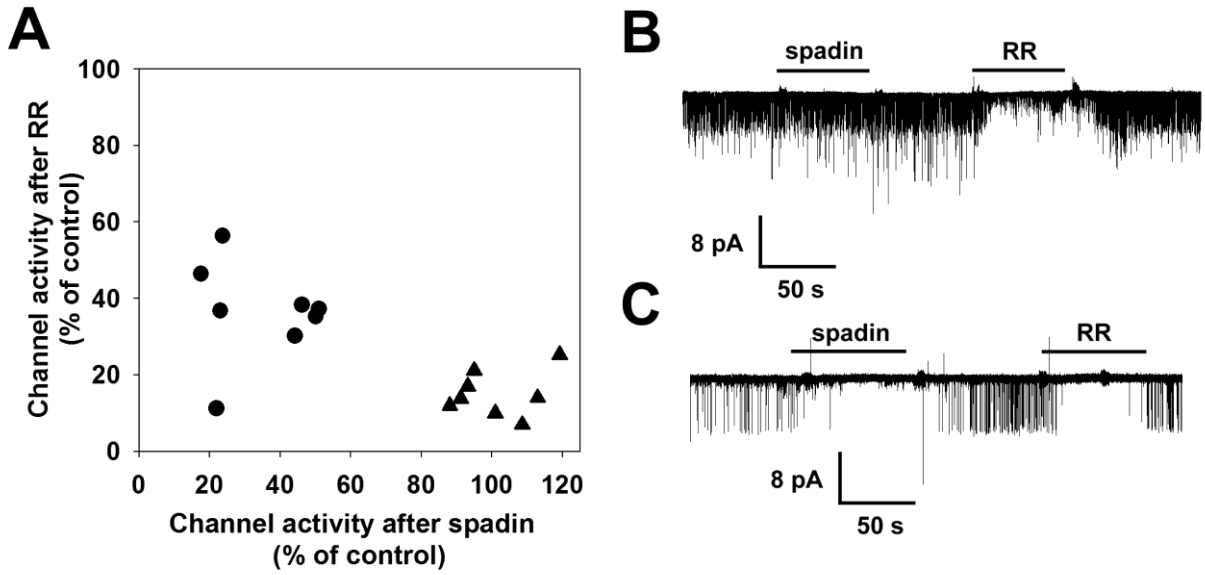

Formation of Functional Heterodimers by TREK-1 and TREK-2 Two-pore Domain Potassium Channel Subunits

Miklós Lengyel, Gábor Czirják and Péter Enyedi

J. Biol. Chem. published online April 28, 2016
